



Fabrication of Cocatalyst NiO-Modified BiVO₄ Composites for Enhanced Photoelectrochemical Performances

Zhi-Qiang Wang^{1*} and HongJun Wang²

¹School of Materials Science and Engineering, North University of China, Taiyuan, China, ²School of Materials Science and Engineering, Jilin University, Changchun, China

OPEN ACCESS

Edited by:

Qingyi Zeng,
University of South China, China

Reviewed by:

Qizhao Wang,
Chang'an University, China
Min Wang,
Jinan University, China
Ligang Xia,
Shanghai University of Electric Power,
China

*Correspondence:

Zhi-Qiang Wang
Zhiqiang_Wang2021@126.com

Specialty section:

This article was submitted to
Inorganic Chemistry,
a section of the journal
Frontiers in Chemistry

Received: 28 January 2022

Accepted: 18 March 2022

Published: 02 June 2022

Citation:

Wang Z-Q and Wang H (2022)
Fabrication of Cocatalyst NiO-Modified
BiVO₄ Composites for Enhanced
Photoelectrochemical Performances.
Front. Chem. 10:864143.
doi: 10.3389/fchem.2022.864143

In this work, NiO modified BiVO₄ (BiVO₄/NiO) nanocomposite was synthesized using hydrothermal and calcination method. The composite of BiVO₄/NiO, further employed as a low-overpotential photoanode, was consisted of BiVO₄ nanoparticles and NiO nanosheets, in which the BiVO₄ nanoelectrode served as the matrix for the attachment of NiO nanosheets. Photoelectrochemical (PEC) tests show that BiVO₄/NiO displayed improved PEC performance compared with pure BiVO₄. The BiVO₄/NiO photoanode delivers a photocurrent density of 1.2 mA/cm² at 1.23 V vs. RHE in a Na₂SO₄ electrolyte under an AM 1.5G solar simulator, which is 0.3 mA/cm² higher than pure BiVO₄ photoanode. Meanwhile, the onset potential also generates a 350 mV cathodic shift. The enhanced performance of the BiVO₄/NiO nanocomposite is attributed to NiO unique lamellar structure capable of providing a large number of active sites. Measurements of electrochemical impedance spectra (EIS) and the incident photon-to-current efficiency (IPCE) illustrate that the enhanced PEC activities are ascribed to the improved charge carrier separation/transport and the promoted water oxidation kinetics furnished by the decoration of NiO cocatalyst.

Keywords: bismuth vanadate, nickel oxide, photoelectrochemical, cocatalyst, water oxidation

INTRODUCTION

Due to the excessive consumption of fossil energy that results in severe environmental pollution worldwide, the development of clean and sustainable energy technologies has received increasing attention. (Iwase et al., 2011; Guo et al., 2014; Zeng et al., 2021a) Clean hydrogen production is seen as a promising strategy, capable of simultaneously addressing climate change and environmental issues related to fossil fuel combustion. (Wang L. et al., 2018; Fukuzumi et al., 2018; Kim et al., 2018) Photoelectrochemical (PEC) water splitting, capable of directly converting solar energy into chemical energy, is considered a promising technology for converting solar energy into stable chemical energy, thus becoming attractive for reducing pollution associated with energy production. (Zhang J. et al., 2016; Wang and Wang, 2018; Weng et al., 2018; Zeng et al., 2019) In the PEC system, the photoanode acts the role of reaction sites for effective oxygen evolution. (Liu et al., 2014; Roger et al., 2017) In conclusion, the development of efficient photoanode materials is of great significance for constructing a practical PEC water splitting system. Various semiconductors including TiO₂ (Crake et al., 2017; Zeng et al., 2020), ZnO (Han et al., 2015; Hong et al., 2015), α -Fe₂O₃ (Dotan et al., 2011; Huang et al., 2016), WO₃ (Huang et al., 2017; Li et al., 2018), BiVO₄ (Wang

et al., 2017a; Wang Q. et al., 2018) and BiOBr (Wang Z.-Q. et al., 2020) etc. have been developed as photocatalytic materials. Among them, scheelite-monoclinic bismuth vanadate (BiVO_4) has been widely studied for PEC water splitting owing to its relatively narrow band gap of 2.4 eV for visible-light absorption, as well as an appropriate band position for effective water oxidation and high stability. (Malathi et al., 2018) However, the application of BiVO_4 is still restricted by its inherent defects such as low charge transport (Zhou et al., 2018), high charge recombination (Zhang Y. et al., 2016) and slow poor water oxidation kinetics (Zhai et al., 2017). The photocurrent density of the pure BiVO_4 is obviously lower than its theoretical value of 7.5 mA/cm^2 (Xu et al., 2014; Chen, 2015) To overcome these issues, transition metal-based catalysts used as cocatalysts are one of the effective ways to improve the PEC water splitting performance.

Transition metal-based materials, especially (Co., Ni, Fe)-based materials, comparable to precious metals because of their low cost and advanced catalytic performance, are considered to be the most promising OER catalysts. (Zhang Q. et al., 2016; Kuang et al., 2016; Wang Z. et al., 2020) The combination of the OER catalyst and the semiconductor light absorber can not only improve the PEC activity by providing an interface reaction active site that reduces overpotential, but also improve the PEC stability by rapidly consuming photo-generated carriers of semiconductor materials against electrolytes (Zhou et al., 2015). (Trotochaud et al., 2014; Zeng et al., 2021b) Recently, Dai (Kenney et al., 2013; Li et al., 2017) and colleagues deposited an ultra-thin nickel film on the n-type silicon substrate as a physical protective layer. It was found that a 2 nm nickel film played a crucial role in the sustainability of n-type silicon photoanodes in the solar-driven water oxidation process. The ultra-thin nickel was used as a protective layer and a passivation layer, and the natural NiO_x formed during the test was employed as an OER promoter. The $\text{NiO}_x/\text{Ni}/\text{n-Si}$ photoanode can work under constant photocurrent of 10 mA/cm^2 , and still have excellent stability after water oxidation of 80 h. In addition, Lewis (Zhou et al., 2019) and his colleagues introduced an ultra-thin CoO_x film as an intermediate layer between NiO_x layer and n-Si to enhance the interaction between co-catalysts/semiconductors. It was found that further passivation of the CoO_x layer on the n-Si surface can change the initiation. The potential was more negative than $\text{NiO}_x/\text{SiO}_x/\text{n-Si}$ photoanode. $\text{NiO}_x/\text{CoO}_x/\text{SiO}_x/\text{n-Si}$ showed the most negative flat band position, which was related to the barrier height in the semiconductor, and therefore highly improved the separation and collection of charge carriers. The above results indicate that the combination of NiO and other favorable semiconductors can remarkably reduce the overpotential of the photoelectrode.

In this study, a BiVO_4 photoanode, acting the role of photoelectrocatalysis substrate, is synthesised by a electrodeposition-calcination method. On the other hand, a nanosheet structured NiO, playing the performance of the water oxidation cocatalyst to combine with the BiVO_4 photoanode and thus improve the PEC performance, is prepared via a hydrothermal-calcination. Under AM 1.5G sunlight, the BiVO_4/NiO film produced a relatively high

photocurrent density of 1.2 mA/cm^2 at 1.23 V vs. RHE, much higher than that of the pure BiVO_4 film. More importantly, the onset potential is negatively shifted by 350 mV relative to pure BiVO_4 . The special structure of NiO is believed to be beneficial to absorb more incident photons through the light-harvesting effect, thereby enhancing the separation and transport of photo-induced charge carriers. Furthermore, the deposition of NiO cocatalyst on the surface of the BiVO_4 photoanode significantly promotes the water oxidation kinetics.

EXPERIMENTAL

Chemicals

$\text{Bi}(\text{NO}_3)_3 \cdot 5\text{H}_2\text{O}$ (Sinopharm Chemical Reagent Co., Ltd., 99.0%), potassium iodide, ethylene glycol are purchased from chemical reagent co, Ltd. P-benzoquinone (Tianjin Institute of Fine Chemicals, 99.0%). $\text{Ni}(\text{NO}_3)_2 \cdot 6\text{H}_2\text{O}$ (Sinopharm Chemical Reagent Co., Ltd., 99.0%), hexamethylenetetramine (HMTA, Chengdu Cologne Chemicals Co., Ltd., 99.0%), Anhydrous ethanol was purchased from Sinopharm Chemical Reagent Co., Ltd. All aqueous solutions were prepared with deionized water.

Preparation of BiVO_4

The preparation of BiVO_4 was synthesized with reference to previous reported work. Systematically, 50 ml of 0.4 M KI solution was first adjusted to pH 1.7 with 1 M HNO_3 , and then 5 mmol $\text{Bi}(\text{NO}_3)_3 \cdot 5\text{H}_2\text{O}$ was added with rapid stirring until dissolved, resulting in an orange-red mixed solution. Then 20 ml of ethanol containing 4.6 mmol of 1,4-benzoquinone was slowly added dropwise to the above solution and stirred for several tens of minutes. Next, BiOI nanosheets were synthesized in a three-electrode system by electrodeposition. Among them, the platinum electrode was used as the counter electrode, the clean FTO glass was used as the working electrode, and the Ag/AgCl (3.5 M KCl) electrode was used as the reference electrode. Cyclic voltammetry (CV) was used for electrodeposition, and the resulting membrane was rinsed with distilled water to obtain a clean BiOI membrane. Immediately after, 150 μl of 0.2 M vanadyl acetylacetonate ($\text{VO}(\text{acac})_2$) DMSO solution was dropped onto the above BiOI nanosheets. Calcined at 450°C for 2 h at a ramp rate of $2^\circ\text{C}/\text{min}$. The cooled membrane was washed with 1 M NaOH solution to remove excess V_2O_5 from the BiVO_4 electrode.

Preparation of BiVO_4/NiO Photoanode

The BiVO_4/NiO photoanode was prepared by a hydrothermal method. The configuration takes 60 ml of solution in which the volume ratio of deionized water and ethanol solution is 2:1. After ultrasonically mixed uniformly, 1.5 mmol $\text{Ni}(\text{NO}_3)_2 \cdot 6\text{H}_2\text{O}$ and 6 mmol HMTA were added thereto, and stirred until dissolved. Then 20 ml of the above mixture was added to a PTFE-lined stainless steel autoclave (100 ml). And the as-prepared BiVO_4 photoanode was placed obliquely with the conductive side facing upwards, heated at 90°C for 4 h. The photoanode was washed three times with water and ethanol and dried at 60°C for 12 h.

Finally, the BiVO₄/NiO photoanode was obtained after calcination in air with a heating rate of 2°C/min at 300°C for 2 h.

Characterizations

The microscopic morphology of the samples was characterized by scanning electron microscopy (SEM, JSM-6701E). The crystal structure of the as-prepared photoanode was measured by X-ray diffraction (XRD) tests on the X-ray diffractometer (D/MAX-2200/PC). UV-Vis diffuse reflectance spectroscopy was used to investigate the response of the prepared photoelectrode to visible light on a UV-3100 spectrometer.

PEC Characterizations

The photoelectrochemical tests of the as-prepared photoanodes were carried out on a CHI 660D electrochemical workstation. A three-electrode system was used, in which a platinum sheet, Ag/AgCl (3.5 M KCl), and the samples were the counter electrode, the reference electrode and the working electrode, respectively. The electrolyte is 0.5 M Na₂SO₄ solution (pH = 6.86). All tests were performed with FTO backside irradiation at room temperature. The scan rate for linear sweep voltammetry (LSV) was 10 mV s⁻¹. The light intensity was calibrated to 100 mW/cm² with an optical power meter. And the incident photon current efficiency (IPCE) was measured using a 300 W xenon lamp with a monochromator in 0.5 M Na₂SO₄ electrolyte at 1.23 V vs. RHE. The photogenerated photocurrent (J_{abs}) undergo two major losses of charge carriers recombination in bulk and at interface. Hence the measured photocurrent during water oxidation (J_{H_2O}) is expressed as follows:

$$J_{H_2O} = J_{abs} \times \eta_{inj} \times \eta_{sep}$$

where J_{abs} is obtained by integrating the distribution of solar power density $P(\lambda)$ with light absorption $\alpha(\lambda)$ of the photoanode as equation:

$$J_{abs} = e \int_0^{\lambda_{abs}} \alpha(\lambda) \frac{P(\lambda)}{h\nu} d\lambda$$

where $\alpha(\lambda) = 1 - 10^{-A}$, A is the absorbance according to the UV-vis spectrum, $P(\lambda)$ = the distribution of solar power density.

The photocurrent during sodium sulfite oxidation was measured ($J_{SO_3^{2-}}$) in order to calculate charge separation efficiencies. Since the interface charge separation efficiency of sodium sulfite oxidation is almost 100% ($\eta_{sep, SO_3^{2-}} = 1$), the charge separation efficiencies can be calculated as follows:

$$\eta_{inj} = J_{SO_3^{2-}} / J_{abs}$$

$$\eta_{sep} = J_{H_2O} / J_{SO_3^{2-}}$$

RESULTS AND DISCUSSION

Characterization of the BiVO₄/NiO Composite Photoanode

The morphology and elemental compositions of the synthesized BiVO₄, BiVO₄/NiO composite photoanode were studied with

SEM and energy dispersive spectroscopy (EDS) in **Figures 1A–H**. **Figure 1A** exhibits the SEM image of nanoporous BiVO₄ film. **Figure 1B** shows the SEM image of BiVO₄/NiO. NiO nanosheets with size distribution about 5–10 nm are fairly continuous and uniformly loaded on the surface of BiVO₄ in large area. The elemental composition and content of BiVO₄/NiO anodes were further investigated by EDS. **Figure 1C** shows the EDS pattern of BiVO₄/NiO photoanode, the weight percentage of elements present in the BiVO₄/NiO photoanode composites are 39.4%, 31.1%, 18.6% and 10.09% for Bi, O, V and Ni, respectively. No other elements or impurities are found. The elemental composition and distribution in the BiVO₄/NiO photoanode were further observed by EDS elemental mapping (**Figures 1D–H**). The results clarify that the elements of Bi, O, V and Ni are present and uniformly distributed in the BiVO₄/NiO photoanode.

The optical absorption properties of pure BiVO₄ and BiVO₄/NiO films were investigated by UV-Vis diffuse reflectance spectroscopy. It can be seen that BiVO₄ and BiVO₄/NiO show good light absorption properties around 500 nm (**Figure 2A**), corresponding to a band gap of 2.4 eV. Notably, the BiVO₄/NiO sample shows almost the same absorption edge as bare BiVO₄ due to the blocking by the thicker BiVO₄ layer, indicating that coating of NiO almost rarely affects light absorption of BiVO₄/NiO. But the BiVO₄ photocathode loaded with NiO co-catalyst shows the relatively low light absorption capacity. The reason is primarily ascribed to the poor optical transparency of the nickel based cocatalyst. (Zhou et al., 2020)

The XRD pattern characterization reveals that the product is composed of three kinds of materials with distinct crystal structures. **Figure 2B** displays the XRD patterns of BiVO₄ and BiVO₄/NiO nanocomposites. The XRD diffraction peaks of BiVO₄ and BiVO₄/NiO nanocomposites are completely consistent with monoclinic BiVO₄ (JCPDS No. 14-0688) and tetragonal SnO₂ (JCPDS No. 46-1088) derived from FTO substrates. No other impurity phases were detected. The appearance of characteristic diffraction peaks at $2\theta = 43.3^\circ$ is corresponding to the (200) crystal plane of the cubic phase NiO, which can be concluded that the composite sample has been successfully prepared.

Performance of the BiVO₄/NiO Composite Photoanode

In order to explore the effect of supported NiO on the PEC performance, the photoelectrochemical water splitting performance of BiVO₄ photoanode modified by NiO cocatalyst was studied by electrochemical workstation. Linear sweep voltammetry (LSV) curves reflect the water oxidation properties of BiVO₄/NiO and pure BiVO₄. As shown in **Figure 3A**, the photocurrent density of unmodified BiVO₄ at 1.23 V vs. RHE is 0.9 mA/cm² and the onset potential is about 0.58 V vs. RHE, which is due to its unique structure and specific crystal orientation, leading to rapid transfer and separation of photogenerated carriers. After loading the NiO cocatalyst on BiVO₄, the photoelectrode showed significant enhancement at all potentials, obtaining a photocurrent of 1.2 mA/cm² at 1.23 V

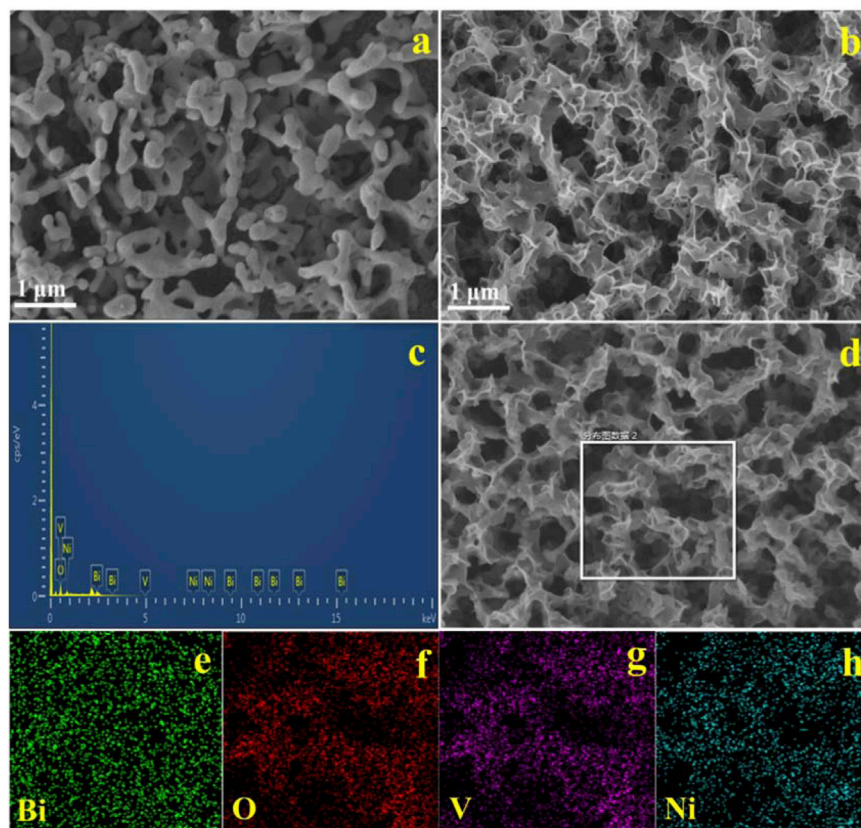


FIGURE 1 | SEM images of the typical samples: (A) BiVO_4 , (B) BiVO_4/NiO , EDS pattern (C) and the EDS elemental mapping (D–H) of as prepared BiVO_4/NiO photoanode.

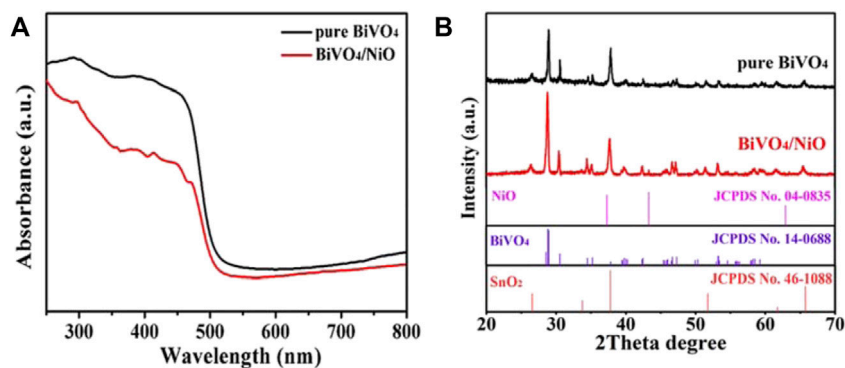


FIGURE 2 | (A) UV–Vis diffuse reflectance spectra of BiVO_4 and BiVO_4/NiO . (B) XRD patterns of the BiVO_4 and BiVO_4/NiO photoanodes.

vs. RHE, which was higher than that of pristine BiVO_4 . In particular, BiVO_4/NiO obtained a more negative onset potential compared to pure BiVO_4 , with a negative shift of about 0.35 V (Figure 3B). The increased photocurrent density and negatively shifted onset potential clearly indicate that the addition of NiO cocatalyst is a feasible way to enhance the water oxidation capacity of BiVO_4 photoanode. Figure 3C shows the chopped photocurrent density–voltage (J – V) curves of $\text{BiVO}_4/$

NiO and pure BiVO_4 . All the photoanodes show an obvious “photo-switching” effect with fast response. Clearly, the BiVO_4/NiO photoanode exhibits a much better PEC performance than BiVO_4 film.

The electron-hole pair recombination and charge generation kinetics of photoanode in PEC water oxidation process can be analyzed by EIS. The photoanode was measured at 1.23 V vs. RHE at AM 1.5G ($100 \text{ mW}/\text{cm}^2$), and the frequency range of the

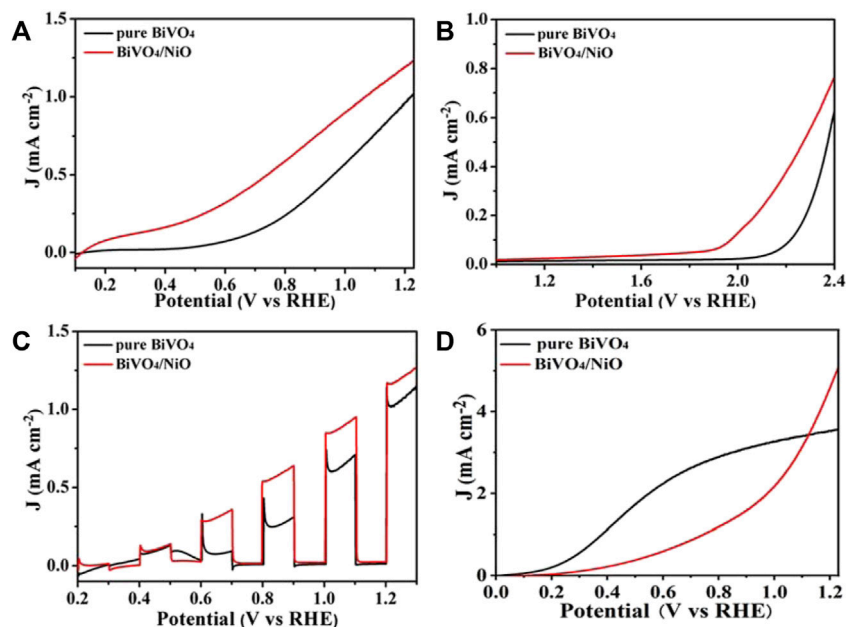


FIGURE 3 | (A) Photocurrent density-voltage curve of BiVO₄ and BiVO₄/NiO photoanodes. **(B)** Photocurrent density-voltage curve of BiVO₄ and BiVO₄/NiO photoanodes in the absence of light. **(C)** Chopped linear sweep photocurrent-potential curve of BiVO₄ and BiVO₄/NiO. **(D)** Sulfite oxidation current curves.

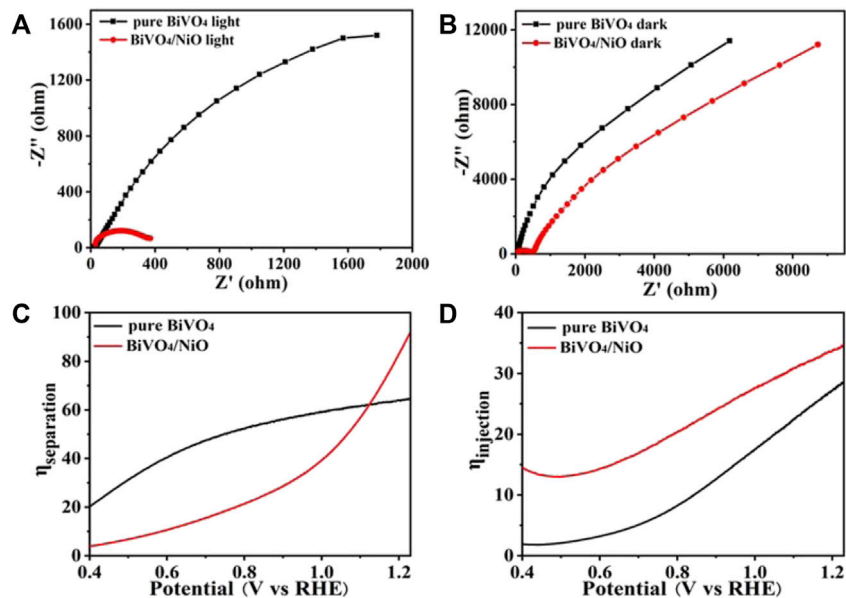


FIGURE 4 | (A) EIS curves of pure BiVO₄ and BiVO₄/NiO under the light, **(B)** and in the dark. The EIS was measured at 1.23 V vs. RHE under an AM 1.5G solar simulator. **(C)** Charge separation efficiency versus potential curves and **(D)** charge injection efficiency versus potential curves of BiVO₄, BiVO₄/NiO.

Nyquist plot was from 100 kHz to 0.1 Hz. The results of impedance spectra are useful for analyzing electrochemical surface reactions. The charge transfer resistance of the photoanode surface is estimated from the small semicircle in the Nyquist diagram, and the smaller the radius, the more effective the separation of charges. In addition, the EIS test

result of dark reaction condition (**Figure 4B**) is consistent with that under light conditions in **Figure 4A**. The BiVO₄/NiO photoanode exhibits the highest charge transportation, suggesting good charge separation ability.

To further explore the charge recombination at the BiVO₄ and BiVO₄/NiO photoanode interfaces, the charge separation and

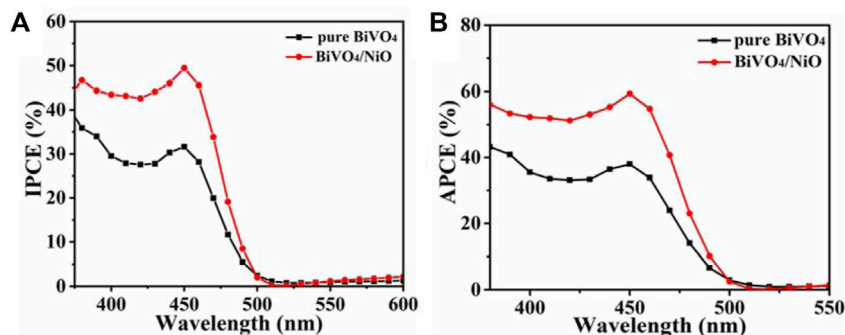


FIGURE 5 | (A) IPCE of BiVO₄, BiVO₄/NiO measured at 1.23 V vs. RHE in the incident wavelength range from 380 to 600 nm. **(B)** APCE spectra for BiVO₄, BiVO₄/NiO photocathodes along with the AM 1.5 irradiance spectrum.

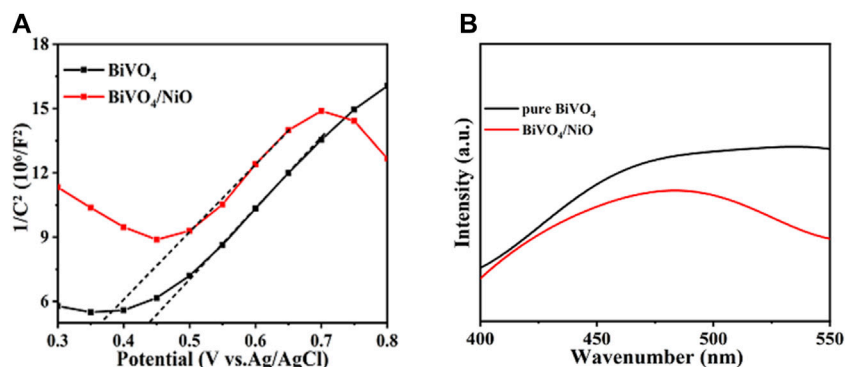


FIGURE 6 | M-S diagram (A) and PL spectra of electrodes **(B)**.

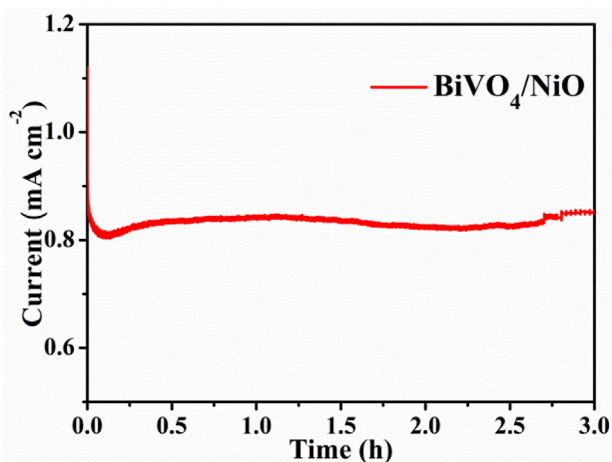
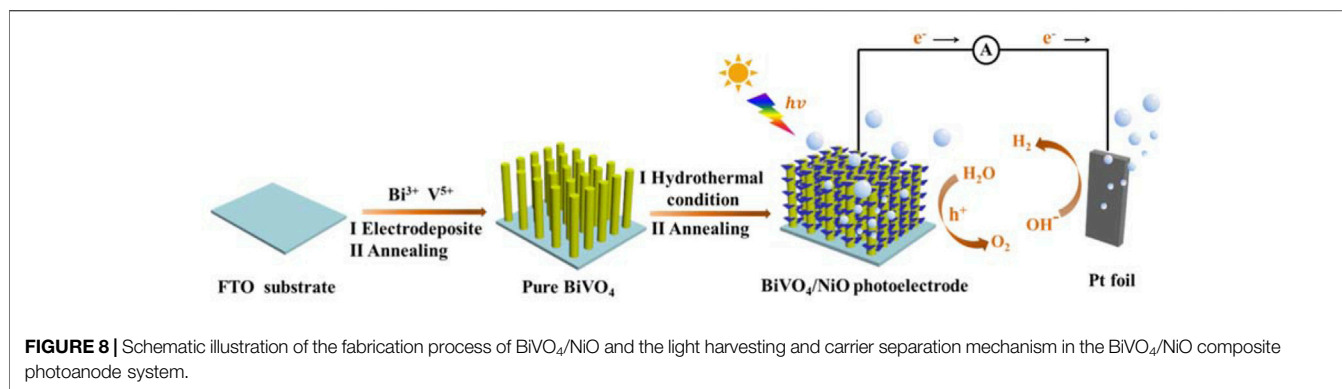


FIGURE 7 | Stability curves of NiO/BiVO₄ photoanode under the same conditions.

injection efficiencies were tested in **Figures 4B,C**. Charge separation efficiency is an important parameter to evaluate the proportion of carriers reaching the electrode surface/electrolyte interface to participate in water oxidation (Wang et al., 2017b).

Therefore, the constant charge separation efficiency is shown in **Figure 3D**, ascribed to the photocurrent density of the BiVO₄/NiO photoanode at an applied potential of 0.6 V vs. RHE when Na₂SO₃ was added to the electrolyte. The separation efficiency of the pure BiVO₄ photoanode increases with the applied potential, especially it can reach about 60% at 1.23 V vs. RHE. However, the BiVO₄/NiO nanostructured array photoanode exhibits a charge separation efficiency of 90% at 1.23 V vs. RHE. From this point of view, the cocatalyst NiO supported on BiVO₄ can significantly improve the charge separation efficiency and facilitate the flow of charge carriers to the electrode surface/electrolyte interface to participate in water oxidation.

The photogenerated holes generated on the surface of the photoanode participate in the water oxidation reaction or recombine with electrons. The charge injection efficiency, defined as the fraction of those holes at the photoanode and electrolyte interface that is used for water oxidation reactions, can be improved by reducing surface recombination or accelerating hole transfer kinetics. (Zhou et al., 2020) As shown in **Figure 4D**, the charge injection efficiency of the pure BiVO₄ photoanode reaches 28% 1.23 V vs. RHE. While the charge injection efficiency of the BiVO₄/NiO photoanode increases to 35% in the potential range of 1.23 V vs. RHE.



The quantum efficiencies of BiVO₄, BiVO₄/NiO photoanodes were determined by measuring incident photon current efficiency (IPCE) and absorbed photon current efficiency (APCE). (Wang et al., 2017b) The calculation of IPCE can refer to the following equation:

$$\text{IPCE} = (J \times 1240) / (P \times \lambda)$$

where J is the current density (mA/cm²) measured at each specific wavelength, λ is the wavelength of the incident light (nm), and P is the power density of the incident light (mW/cm²). As shown in **Figure 5A**, BiVO₄/NiO nanocomposites exhibit slightly higher IPCE values in the 450–500 nm range compared to bare BiVO₄. The PEC performance mainly depends on the light-harvesting efficiency, charge separation efficiency, and collection yield. Since the light-harvesting efficiency is almost unchanged after the modification of the NiO cocatalyst, the enhancement of IPCE may be due to the fast separation of charge carriers and the accelerated water oxidation kinetics of the reaction, resulting in the enhanced photocurrent. The IPCE results are consistent with the above J-V measurements.

To obtain the absorbed photon-current efficiency, the APCE value of the photoanode was measured at 0.6 V vs. RHE, as shown in **Figure 5B**. The APCE value of BiVO₄/NiO photoanode is significantly higher than that of BiVO₄ from 380 to 500 nm, which is consistent with the overall PEC performance.

Figure 6A shows the Mott Schottky barrier of BiVO₄ and BiVO₄/NiO. The capacitance-voltage curve is usually used to analyze the reasons for the enhancement of semiconductor performance. In order to better study the reasons for the increase of photocurrent after supporting the cocatalyst. Therefore, the capacitance-voltage curves of BiVO₄ and BiVO₄/NiO electrodes were measured under dark reaction conditions, and the x -axis tangent was made on the curves of BiVO₄ and BiVO₄/NiO. The tangent was positive, indicating that BiVO₄ and BiVO₄/NiO are both n-type semiconductors. The smaller slope of the composite electrode, the greater the carrier density. Thus, the BiVO₄/NiO electrode has the largest carrier density. The increased carrier density causes the conductivity of BiVO₄ to increase and ultimately increases its photocurrent density. Fluorescence spectroscopy (PL) can be used to effectively analyze the separation and recombination effects of photogenerated carriers. As shown in **Figure 6B**, it can be observed that the peak intensity of the BiVO₄/NiO electrode is weaker than that of the pure BiVO₄

electrode, which indicates that after NiO is loaded on the BiVO₄ surface, the recombination rate of photo-generated electrons and holes becomes slower and the charge separation efficiency is improved.

Stability test is an important index parameter to evaluate the effect of photoelectric catalyst and whether it has application value. The stability test of the BiVO₄/NiO photoanode was analyzed under continuous irradiation under AM 1.5G. As shown in **Figure 7**, it can be observed that under the continuous irradiation of 3 h, the photocurrent density of the NiO/BiVO₄ electrode is not significantly attenuated, indicating that the stability of the BiVO₄ photoanode can be improved after loading NiO.

DISCUSSION ON MECHANISM

Based on above results, the possible mechanisms for the enhancement in photoelectrocatalytic activity of BiVO₄/NiO composite photoanode and the specific photogenerated charge carriers transfer are shown in **Figure 8**. In BiVO₄ with monoclinic scheelite structure, the Bi 6s and O 2p orbitals hybridize to form the valence band. When the BiVO₄/NiO composite is irradiated with visible light, electron-hole pairs are generated in BiVO₄, in which electrons in the valence band are excited to the conduction band and holes stay in the conduction band. With the NiO coated on the surface of BiVO₄, NiO as a cocatalyst regulates the built-in electric field of BiVO₄ photocatalyst, accelerates the charge separation rate of BiVO₄, and thus the PEC performance of BiVO₄ is improved.

CONCLUSION

In conclusion, we successfully fabricated an efficient nanostructured BiVO₄/NiO photoanode by a two-step method of hydrothermal calcination synthesis. The PEC performance of the NiO-modified BiVO₄ photoanode was improved in 0.5 M Na₂SO₄ (pH = 6.86) electrolyte, reaching 1.2 mA/cm² at 1.23 V vs. RHE, higher than that of the pure BiVO₄ sample. In particular, the onset potential of the composite photoanode has a significant negative shift. The excellent PEC performance could be attributed to NiO abundant nano flake structure, the improved charge separation/transport efficiency and accelerated water oxidation kinetics thanks to the deposited NiO

cocatalyst. Our work shed a light for design and fabrication of nanostructured photoelectrode with efficient PEC performances.

DATA AVAILABILITY STATEMENT

The original contributions presented in the study are included in the article/Supplementary Material, further inquiries can be directed to the corresponding author.

REFERENCES

- Chen, P. (2015). A Promising Strategy to Fabricate the Cu/BiVO₄ Photocatalysts and Their Enhanced Visible-Light-Driven Photocatalytic Activities. *J. Mater. Sci. Mater. Electron.* 27 (3), 2394–2403. doi:10.1007/s10854-015-4037-5
- Crake, A., Christoforidis, K. C., Kafzas, A., Zafeiratos, S., and Petit, C. (2017). CO₂ Capture and Photocatalytic Reduction Using Bifunctional TiO₂/MOF Nanocomposites under UV-Vis Irradiation. *Appl. Catal. B: Environ.* 210, 131–140. doi:10.1016/j.apcatb.2017.03.039
- Dotan, H., Sivula, K., Grätzel, M., Rothschild, A., and Warren, S. C. (2011). Probing the Photoelectrochemical Properties of Hematite (α -Fe₂O₃) Electrodes Using Hydrogen Peroxide as a Hole Scavenger. *Energy Environ. Sci.* 4 (3), 958–964. doi:10.1039/c0ee00570c
- Fukuzumi, S., Lee, Y.-M., and Nam, W. (2018). Thermal and Photocatalytic Production of Hydrogen with Earth-Abundant Metal Complexes. *Coord. Chem. Rev.* 355, 54–73. doi:10.1016/j.ccr.2017.07.014
- Guo, K., Liu, Z., Zhou, C., Han, J., Zhao, Y., Liu, Z., et al. (2014). Fabrication of TiO₂ Nano-Branched arrays/Cu₂S Composite Structure and its Photoelectric Performance. *Appl. Catal. B: Environ.* 154–155, 27–35. doi:10.1016/j.apcatb.2014.02.004
- Han, J., Liu, Z., Guo, K., Wang, B., Zhang, X., and Hong, T. (2015). High-efficiency Photoelectrochemical Electrodes Based on ZnIn₂S₄ Sensitized ZnO Nanotube Arrays. *Appl. Catal. B: Environ.* 163, 179–188. doi:10.1016/j.apcatb.2014.07.040
- Hong, T., Liu, Z., Liu, H., Liu, J., Zhang, X., Han, J., et al. (2015). Preparation and Enhanced Photoelectrochemical Performance of Selenite-Sensitized Zinc Oxide Core/shell Composite Structure. *J. Mater. Chem. A* 3 (8), 4239–4247. doi:10.1039/c4ta05973e
- Huang, J., Hu, G., Ding, Y., Pang, M., and Ma, B. (2016). Mn-doping and NiFe Layered Double Hydroxide Coating: Effective Approaches to Enhancing the Performance of α -Fe₂O₃ in Photoelectrochemical Water Oxidation. *J. Catal.* 340, 261–269. doi:10.1016/j.jcat.2016.05.007
- Huang, J., Zhang, Y., and Ding, Y. (2017). Rationally Designed/Constructed CoOx/WO₃ Anode for Efficient Photoelectrochemical Water Oxidation. *ACS Catal.* 7 (3), 1841–1845. doi:10.1021/acscatal.7b00022
- Iwase, A., Ng, Y. H., Ishiguro, Y., Kudo, A., and Amal, R. (2011). Reduced Graphene Oxide as a Solid-State Electron Mediator in Z-Scheme Photocatalytic Water Splitting under Visible Light. *J. Am. Chem. Soc.* 133 (29), 11054–11057. doi:10.1021/ja203296z
- Kenney, M. J., Gong, M., Li, Y., Wu, J. Z., Feng, J., Lanza, M., et al. (2013). High-performance Silicon Photoanodes Passivated with Ultrathin Nickel Films for Water Oxidation. *Science* 342 (6160), 836–840. doi:10.1126/science.1241327
- Kim, C.-H., Han, J.-Y., Lim, H., Lee, K.-Y., and Ryi, S.-K. (2018). Hydrogen Production by Steam Methane Reforming in Membrane Reactor Equipped with Pd Membrane Deposited on NiO/YSZ/NiO Multilayer-Treated Porous Stainless Steel. *J. Membr. Sci.* 563, 75–82. doi:10.1016/j.memsci.2018.05.037
- Kuang, Y., Jia, Q., Nishiyama, H., Yamada, T., Kudo, A., and Domen, K. (2016). A Front-Illuminated Nanostructured Transparent BiVO₄ Photoanode for >2% Efficient Water Splitting. *Adv. Energy Mater.* 6, 1501645. doi:10.1002/aenm.201501645
- Li, L., Xiao, S., Li, R., Cao, Y., Chen, Y., Li, Z., et al. (2018). Nanotube Array-like WO₃ Photoanode with Dual-Layer Oxygen-Evolution Cocatalysts for Photoelectrocatalytic Overall Water Splitting. *ACS Appl. Energy Mater.* 1 (12), 6871–6880. doi:10.1021/acsaem.8b01215
- Li, S., Chen, Z., Kong, W., Jia, X., Cai, J., and Dong, S. (2017). Effect of Polyethylene Glycol on the NiO Photocathode. *Nanoscale Res. Lett.* 12, 501. doi:10.1186/s11671-017-2267-6

AUTHOR CONTRIBUTIONS

Z-QW: Writing—review and editing. HJW: Methodology.

FUNDING

This work was financially supported by the National Natural Science Foundation of China (Nos. 51773184 and U1810114).

- Liu, Z., Guo, K., Han, J., Li, Y., Cui, T., Wang, B., et al. (2014). Dendritic TiO₂/In₂S₃/AgInS₂ Trilaminar Core-Shell Branched Nanoarrays and the Enhanced Activity for Photoelectrochemical Water Splitting. *Small* 10 (15), 3153–3161. doi:10.1002/sml.201400622
- Malathi, A., Madhavan, J., Ashokkumar, M., and Arunachalam, P. (2018). A Review on BiVO₄ Photocatalyst: Activity Enhancement Methods for Solar Photocatalytic Applications. *Appl. Catal. A: Gen.* 555, 47–74. doi:10.1016/j.apcata.2018.02.010
- Roger, I., Shipman, M. A., and Symes, M. D. (2017). Earth-abundant Catalysts for Electrochemical and Photoelectrochemical Water Splitting. *Nat. Rev. Chem.* 1 (1), 0003. doi:10.1038/s41570-016-0003
- Trotochaud, L., Young, S. L., Ranney, J. K., and Boettcher, S. W. (2014). Nickel-Iron Oxyhydroxide Oxygen-Evolution Electrocatalysts: The Role of Intentional and Incidental Iron Incorporation. *J. Am. Chem. Soc.* 136 (18), 6744–6753. doi:10.1021/ja502379c
- Wang, L., Duan, S., Jin, P., She, H., Huang, J., Lei, Z., et al. (2018). Anchored Cu(II) Tetra(4-Carboxylphenyl)porphyrin to P25 (TiO₂) for Efficient Photocatalytic Ability in CO₂ Reduction. *Appl. Catal. B: Environ.* 239, 599–608. doi:10.1016/j.apcatb.2018.08.007
- Wang, Q., He, J., Shi, Y., Zhang, S., Niu, T., She, H., et al. (2017b). Designing non-noble/semiconductor Bi/BiVO₄ Photoelectrode for the Enhanced Photoelectrochemical Performance. *Chem. Eng. J.* 326, 411–418. doi:10.1016/j.cej.2017.05.171
- Wang, Q., He, J., Shi, Y., Zhang, S., Niu, T., She, H., et al. (2017a). Synthesis of MFe₂O₄ (M = Ni, Co)/BiVO₄ Film for Photoelectrochemical Hydrogen Production Activity. *Appl. Catal. B: Environ.* 214, 158–167. doi:10.1016/j.apcatb.2017.05.044
- Wang, Q., Niu, T., Wang, L., Yan, C., Huang, J., He, J., et al. (2018). FeF₂/BiVO₄ Heterojunction Photoelectrodes and Evaluation of its Photoelectrochemical Performance for Water Splitting. *Chem. Eng. J.* 337, 506–514. doi:10.1016/j.cej.2017.12.126
- Wang, Z.-Q., Wang, H., Wu, X.-F., and Chang, T.-L. (2020). Oxygen Vacancies and P-N Heterojunction Modified BiOBr for Enhancing Donor Density and Separation Efficiency under Visible-Light Irradiation. *J. Alloys Compd.* 834, 155025. doi:10.1016/j.jallcom.2020.155025
- Wang, Z., Lei, Q., Wang, Z., Yuan, H., Cao, L., Qin, N., et al. (2020). In-situ Synthesis of Free-Standing Feni-Oxyhydroxide Nanosheets as a Highly Efficient Electrocatalyst for Water Oxidation. *Chem. Eng. J.* 395, 125180. doi:10.1016/j.cej.2020.125180
- Wang, Z., and Wang, L. (2018). Photoelectrode for Water Splitting: Materials, Fabrication and Characterization. *Sci. China Mater.* 61 (6), 806–821. doi:10.1007/s40843-018-9240-y
- Weng, B., Grice, C. R., Meng, W., Guan, L., Xu, F., Yu, Y., et al. (2018). Metal-Organic Framework-Derived CoWP@C Composite Nanowire Electrocatalyst for Efficient Water Splitting. *ACS Energy Lett.* 3 (6), 1434–1442. doi:10.1021/acscenergylett.8b00584
- Xu, X., Zou, Q., Yuan, Y., Ji, F., Fan, Z., and Zhou, B. (2014). Preparation of BiVO₄-Graphene Nanocomposites and Their Photocatalytic Activity. *J. Nanomater.* 2014, 1–6. doi:10.1155/2014/401697
- Zeng, Q., Chang, S., Beyhaqi, A., Lian, S., Xu, H., Xie, J., et al. (2020). Efficient Solar Hydrogen Production Coupled with Organics Degradation by a Hybrid Tandem Photocatalytic Fuel Cell Using a Silicon-Doped TiO₂ Nanorod Array with Enhanced Electronic Properties. *J. Hazard. Mater.* 394, 121425. doi:10.1016/j.jhazmat.2019.121425
- Zeng, Q., Chang, S., Beyhaqi, A., Wang, M., and Hu, C. (2019). Efficient Electricity Production Coupled with Water Treatment via a Highly Adaptable, Successive

- Water-Energy Synergistic System. *Nano Energy* 67, 104237. doi:10.1016/j.nanoen.2019.104237
- Zeng, Q., Chang, S., Wang, M., Li, M., Deng, Q., Xiong, Z., et al. (2021a). Highly-active, Metal-free, Carbon-Based ORR Cathode for Efficient Organics Removal and Electricity Generation in a PFC System. *Chin. Chem. Lett.* 32 (7), 2212–2216. doi:10.1016/j.ccllet.2020.12.062
- Zeng, Q., Fu, X., Chang, S., Zhang, Q., Xiong, Z., Liu, Y., et al. (2021b). Ordered Ti-Doped FeVO₄ Nanoblock Photoanode with Improved Charge Properties for Efficient Solar Water Splitting. *J. Colloid Interf. Sci.* 604, 562–567. doi:10.1016/j.jcis.2021.07.037
- Zhai, Y., Yin, Y., Liu, X., Li, Y., Wang, J., Liu, C., et al. (2017). Novel Magnetically Separable BiVO₄/Fe₃O₄ Photocatalyst: Synthesis and Photocatalytic Performance under Visible-Light Irradiation. *Mater. Res. Bull.* 89, 297–306. doi:10.1016/j.materresbull.2017.01.011
- Zhang, J., Liu, Z., and Liu, Z. (2016). Novel WO₃/Sb₂S₃ Heterojunction Photocatalyst Based on WO₃ of Different Morphologies for Enhanced Efficiency in Photoelectrochemical Water Splitting. *ACS Appl. Mater. Inter.* 8 (15), 9684–9691. doi:10.1021/acscami.6b00429
- Zhang, Q., Li, Z., Wang, S., Li, R., Zhang, X., Liang, Z., Han, H., et al. (2016). The Effect of Redox Cocatalysts Location on Photocatalytic Overall Water Splitting over Cubic NaTaO₃ Semiconductor Crystals Exposed with Equivalent Facets. *ACS Catal.* 4, 2182–2191. doi:10.1021/acscatal.5b02503
- Zhang, Y., Wang, D., Zhang, X., Chen, Y., Kong, L., Chen, P., et al. (2016). Enhanced Photoelectrochemical Performance of Nanoporous BiVO₄ Photoanode by Combining Surface Deposited Cobalt-Phosphate with Hydrogenation Treatment. *Electrochimica Acta* 195, 51–58. doi:10.1016/j.electacta.2016.02.137
- Zhou, C., Wang, S., Zhao, Z., Shi, Z., Yan, S., and Zou, Z. (2018). A Facet-dependent Schottky-Junction Electron Shuttle in a BiVO₄{010}-Au-Cu₂O Z-Scheme Photocatalyst for Efficient Charge Separation. *Adv. Funct. Mater.* 28 (31), 1801214. doi:10.1002/adfm.201801214
- Zhou, S., Chen, K., Huang, J., Wang, L., Zhang, M., Bai, B., et al. (2020). Preparation of Heterometallic CoNi-MOFs-Modified BiVO₄: a Steady Photoanode for Improved Performance in Photoelectrochemical Water Splitting. *Appl. Catal. B: Environ.* 266, 118513. doi:10.1016/j.apcatb.2019.118513
- Zhou, S., Yue, P., Huang, J., Wang, L., She, H., and Wang, Q. (2019). High-performance Photoelectrochemical Water Splitting of BiVO₄@Co-MIm Prepared by a Facile *In-Situ* Deposition Method. *Chem. Eng. J.* 371, 885–892. doi:10.1016/j.cej.2019.04.124
- Zhou, X., Liu, R., Sun, K., Friedrich, D., McDowell, M. T., Yang, F., et al. (2015). Interface Engineering of the Photoelectrochemical Performance of Ni-Oxide-Coated n-Si Photoanodes by Atomic-Layer Deposition of Ultrathin Films of Cobalt Oxide. *Energ. Environ. Sci.* 8, 2644–2649. doi:10.1039/c5ee01687h

Conflict of Interest: The authors declare that the research was conducted in the absence of any commercial or financial relationships that could be construed as a potential conflict of interest.

Publisher's Note: All claims expressed in this article are solely those of the authors and do not necessarily represent those of their affiliated organizations, or those of the publisher, the editors and the reviewers. Any product that may be evaluated in this article, or claim that may be made by its manufacturer, is not guaranteed or endorsed by the publisher.

Copyright © 2022 Wang and Wang. This is an open-access article distributed under the terms of the Creative Commons Attribution License (CC BY). The use, distribution or reproduction in other forums is permitted, provided the original author(s) and the copyright owner(s) are credited and that the original publication in this journal is cited, in accordance with accepted academic practice. No use, distribution or reproduction is permitted which does not comply with these terms.